Journal of Hazardous Materials 182 (2010) 90–96

Contents lists available at ScienceDirect

Journal of Hazardous Materials

journal homepage: www.elsevier.com/locate/jhazmat

Nitrogen-doped TiO_2 modified with NH_4F for efficient photocatalytic degradation of formaldehyde under blue light-emitting diodes

Yuexiang Li [a,*], Yuan Jiang [a], Shaoqin Peng [a], Fengyi Jiang [b]

[a] Department of Chemistry, Nanchang University, Xuefu Road 999, Nanchang 330031, PR China
[b] Institute of Materials Science, Nanchang University, Nanjing Road 245, Nanchang 330047, PR China

ARTICLE INFO

Article history:
Received 30 November 2009
Received in revised form 31 May 2010
Accepted 1 June 2010
Available online 8 June 2010

Keywords:
Photocatalysis
Formaldehyde
Blue LED
TiO_2
F-N-codoping

ABSTRACT

A nitrogen-doped TiO_2 (N-TiO_2) photocatalyst was prepared by calcination of the hydrolysis precipitate of $Ti(SO_4)_2$ with aqueous ammonia. The prepared N-TiO_2 was treated with NH_4F (F-N-TiO_2) by an impregnation-calcination method. The photocatalyst (F-N-TiO_2) was characterized by X-ray diffraction (XRD), Fourier Transform Infrared (FT-IR), UV–vis diffusive reflectance spectroscopy (DRS), BET and X-ray photoelectron spectroscopy (XPS). With blue light-emitting diode (LED) as the light source, its photocatalytic activity for the degradation of formaldehyde was investigated. NH_4F treatment enhances markedly photocatalytic activity of N-TiO_2. The treatment increases the visible absorption of N-TiO_2, decreases its specific surface area and influences the concentration of oxygen vacancies in N-TiO_2. Photocatalytic activity of F-N-TiO_2 depends on the visible absorption, the specific surface area, and the concentration of oxygen vacancies. The preparation conditions, such as the calcination temperature and the initial molar ratio of NH_4F to N-TiO_2, have a significant influence on the photocatalytic activity. The doping mechanism of NH_4F was investigated.

1. Introduction

Formaldehyde is a common indoor air pollutant. Photocatalytic degradation of volatile organic compounds, including formaldehyde, is one of the most popular approaches of indoor air pollution control. However, most studies have focused on utilization of ultraviolet light sources using TiO_2 as photocatalysts [1]. Preparation of TiO_2 with visible-light activity is very important to the application of indoor light sources and sunlight. In recent years, a number of studies have reported that TiO_2 doped with metal or non-metal compounds exhibit visible-light activity [2–9]. Among them, nitrogen doping has been considered to be one of the most effective means for producing visible irradiation effect [2–4].

Many methods have been documented to successfully prepare N-doped TiO_2 photocatalysts (N-TiO_2): hydrolysis of organic and inorganic titanium compounds with ammonia water followed by heating the resultant precipitates or their mixtures with urea [4,10], nitridation of TiO_2 colloidal nanoparticles with alkylammonium salts at room temperature [11,12], mechanochemical reaction of titania with hexamethylenetetramine or urea [13], spray pyrolysis from a mixed aqueous solution containing $TiCl_4$ and a N precursor [14], heat treatment of a TiO_2 precursor in an ammonia atmosphere [15] and oxidation of titanium nitride[16]. Among the above methods, annealing of the hydrolysis precipitate of titanium compounds with ammonia water is the simplest and most applicable process. However, the photocatalytic activity of N-TiO_2 is low because nitrogen doping into TiO_2 can produce oxygen vacancies in TiO_2 lattice [17]. Doping of a second species in N-TiO_2, such as B^{3+}, can remove the vacancies and thus enhance the activity [6].

Fluorine doping into TiO_2 is also effective for enhancing the photocatalytic activity of TiO_2 [18,19]. Yu et al. [18] proposed that the doped F^- ions converted Ti^{4+} to Ti^{3+} by charge compensation. A certain amount of the Ti^{3+} reduced electron–hole recombination rate and thus enhanced the photocatalytic activity. Hattori et al. [19] interpreted that the enhancement of photocatalytic activity was mainly ascribable to the improvement of TiO_2 crystallinity caused by F-doping. Doping of F^- ions into N-TiO_2 should reduce the vacancies by charge compensation, which could enhance its photocatalytic activity.

A light-emitting diode (LED) is a new electronic light source with many advantages over traditional light sources including lower energy consumption, longer lifetime, smaller size, and faster switching. LEDs are used not only as low-energy indicators but also for replacements for traditional (indoor/outdoor) light sources.

Photocatalytic activity of semiconductors is due to the production of excited electrons in the conduction band of the semiconductors, along with corresponding positive holes in the valence band by the absorption of light. These energetically

* Corresponding author. Tel.: +86 791 3969983; fax: +86 791 3969983.
E-mail address: liyx@ncu.edu.cn (Y. Li).

0304-3894/$ – see front matter © 2010 Elsevier B.V. All rights reserved.
doi:10.1016/j.jhazmat.2010.06.002

excited species are mobile and capable of initiating many chemical reactions usually by the production of radical species at the semiconductor surface. Thus, a photocatalyst with a stronger ability for light absorption should exhibit higher photocatalytic activity. On the other hand, recombination of the photogenerated electrons and holes can occur very quickly, dissipating the input energy as heat [20]. Suitable surface defects can enhance photocatalytic activity of TiO_2, while bulk defects decrease the activity [21].

In the present study, a nitrogen-doped TiO_2 (N-TiO_2) photocatalyst was prepared by calcination of the hydrolysis precipitate of $Ti(SO_4)_2$ with aqueous ammonia. The prepared N-TiO_2 was modified with NH_4F by an impregnation-calcination method. With blue LEDs as the light source, the photocatalytic activity of the modified N-TiO_2 for the degradation of formaldehyde was investigated. To the best of our knowledge, effects of the NH_4F treatment on N-TiO_2 have not been reported. The photocatalyst was characterized by various techniques, and the photocatalytic mechanism is discussed.

2. Experimental

2.1. Preparation of photocatalysts and their films

In this work, except for titanium sulfate (TS) and paraformaldehyde, which were of chemical reagent grade, the other chemicals were of analytic reagent grade and were used without any further purification.

24.0 g TS was dissolved in 200 ml distilled water under strong stirring. The pH of the TS solution was adjusted to 7.2 with concentrated aqueous ammonia (28 wt%) to produce white precipitate (the hydrolysis product of TS). After standing for 10 h, the hydrolysis product was filtrated and washed with distilled water to remove SO_4^{2-} (determined with saturated $BaCl_2$ solution). The sample was then dried at 60 °C for 10 h and milled in a mortar. Finally, the sample was calcined at 300 °C for 2 h to obtain N-doped TiO_2 (denoted as N-TiO_2). Pure TiO_2 was prepared by the same method for N-TiO_2 except for using 1.0 mol L^{-1} NaOH solution as a precipitator.

N-TiO_2 modified with NH_4F (F-N-TiO_2) was prepared by the following process: 1.0 g N-TiO_2 and a given amount of NH_4F were dispersed in 4.0 ml distilled water in an ultrasonic bath for 40 min. After standing for 10 h, the mixture was dried at 60 °C for 12 h. The sample was calcined at given temperatures (300, 400 and 550 °C respectively) for 2 h to obtain F-N-TiO_2. This sample was denoted as F-N-TiO_2(a:b)-temperature, where a:b represents the calculated initial molar ratio of NH_4F to N-TiO_2. For comparison purpose, N-TiO_2 modified with NH_4Cl in a 1:6 ratio of NH_4Cl to N-TiO_2, was prepared at 300 °C by the same process for F-N-TiO_2(1:6)-300. The sample was denoted as NH_4Cl-N-TiO_2(1:6)-300. Three other samples: TiO_2 modified with NH_4Cl, NH_4F, and NaF respectively in 1:6 ratios of NH_4Cl, NH_4F and NaF to TiO_2, were prepared by the same method at 300 °C. They were denoted as NH_4Cl-TiO_2(1:6)-300, NH_4F-TiO_2(1:6)-300 and NaF-TiO_2(1:6)-300 respectively. In order to compare the performance of F-N-TiO_2 with that of N-TiO_2, N-TiO_2 was treated by the same process for F-N-TiO_2(1:6)-300 with distilled water. The sample was denoted as N-TiO_2 (4 h).

Photocatalyst film was prepared by the following process: a ca. 31.6 cm^2 square glass was cleaned by heating in an aqueous NaOH solution, washed with distilled water and ethanol by ultrasonication and then dried at room temperature. 0.020 g of the above photocatalyst was dispersed in 2.0 ml distilled water in an ultrasonic bath for 40 min. The resultant suspension was spread on the glass, and dried at room temperature to obtain the photocatalyst film.

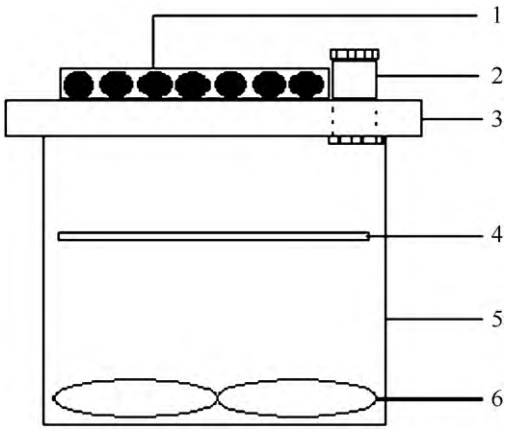

Fig. 1. Experimental setup for photocatalytic decomposition of formaldehyde: (1) light source (blue LEDs), (2) sampling/injection port, (3) organic glass plate, (4) a glass plate with photocatalyst film, (5) stainless steel vessel and (6) electric fan.

2.2. Characterization of photocatalyst

XRD patterns were measured on a Britain Bede D1 System multifunction X-ray diffractometer using Cu Kα radiation: λ = 0.15406 nm. UV–vis DRS spectra were obtained on a HITACHI U-3310 spectrophotometer equipped with an integrating sphere accessory ($BaSO_4$ was used as a reference). IR spectra of the prepared photocatalysts were measured on a Nicolet 380 FT-IR spectrometer by the transmission method using the KBr pellet technique. XPS spectra were measured on an UG-ESCALAB 210 X-ray photoelectron spectroscope equipped with Mg Kα excitation. The C 1s peak, set at 285.0 eV, was used as an internal reference for absolute binding energy. The BET specific surface area of the samples was obtained on a Micromeritics Chemisorb 2750 analyzer by BET method using nitrogen as adsorbent. The average photon flux of incident light was determined on a FGH-1 Ray virtual radiation actinometer (light spectrum: 400–700 nm).

2.3. Photocatalytic activity

Standard formaldehyde gas was prepared by the following process: 0.50 g paraformaldehyde was added to a ca. 190 ml Pyrex cell. The cell was heated to 50 °C with an electric heating jacket and then the temperature was kept for 10 h. The concentration of formaldehyde in the headspace of the cell was 62.4 ± 0.5 μg ml^{-1}. The top of the cell was sealed with a silicone rubber septum. Sampling was made through the septum.

Photocatalytic reactions were conducted in a ca. 578 ml self-made closed cylindrical stainless steel cell with an organic glass cover (Fig. 1). A group of LEDs (λ_{max} = 458 nm, Latticepower Co., Ltd, China) embedded into a panel was used as the light source. The incident intensity of the light to the film surface position was ca. 1.39 mW cm^{-2} s^{-1}. 20 ml of the formaldehyde gas was added to the cell through the sampling/injection port. The electric fan was kept on for 30 min and then the light source was turned on. The sampling/injection port was sealed with a silicone rubber septum. Sampling was made intermittently through the septum during experiments. The photocatalytic activity was determined by measuring the amount of formaldehyde, which was determined quantitatively using the acetylacetone spectrophotometric method [22]. The degradation rate of formaldehyde was estimated by the following equation:

$$D(\%) = \frac{C_0 - C}{C_0} \times 100 \quad (1)$$

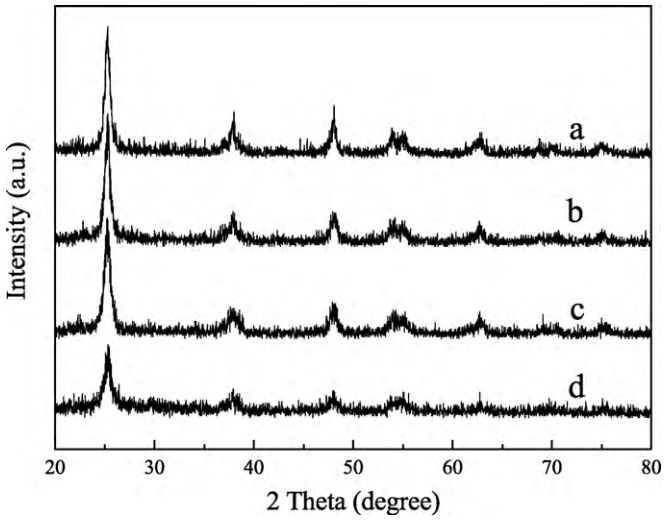

Fig. 2. XRD patterns of various samples calcined at 300 °C. (a) F-N-TiO_2(1:6)-300, (b) N-TiO_2 (4 h), (c) N-TiO_2 and (d)TiO_2.

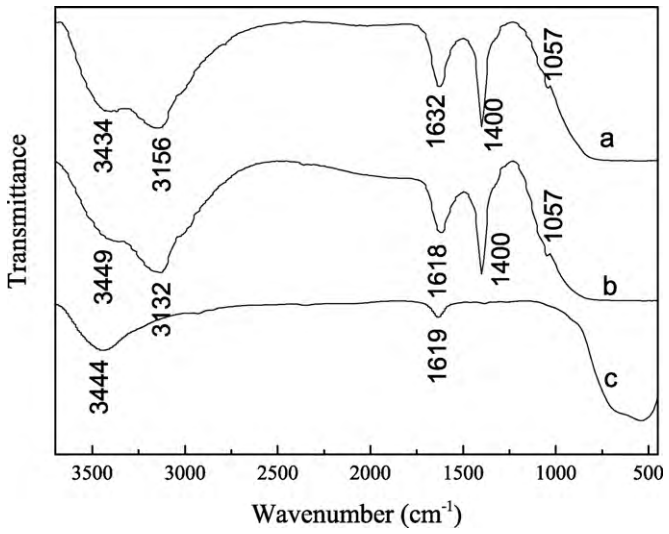

Fig. 3. FT-IR spectra of various samples calcined at 300 °C. (a) F-N-TiO_2(1:6), (b) N-TiO_2 (4 h) and (c) TiO_2.

where C_0 represents the initial concentration of formaldehyde, and C represents the measured concentration.

3. Results

3.1. Performance of F-N-TiO_2(a:b)-300 and its photoactivity

3.1.1. Structure and specific surface

Fig. 2 shows XRD patterns of TiO_2, N-TiO_2, N-TiO_2 (4 h) and F-N-TiO_2(1:6)-300. All the catalysts calcined at 300 °C are in anatase phase. No nitrogen and fluorine-derived peaks were detected for F-N-TiO_2(1:6)-300. This resulted from the low doping contents of nitrogen and fluorine and high dispersion of nitrogen and fluorine in TiO_2 particles.

The crystalline size (Table 1), D, was calculated by following Scherrer's formula [4]:

$$D = \frac{0.9\lambda}{\beta_{1/2}\ \cos\theta} \quad (2)$$

where λ is the wavelength (nm) of the applied characteristic X-ray (λ = 0.15406 nm), $\beta_{1/2}$ is the half-value width of anatase (1 0 1) peak obtained by XRD, and θ is 25.3/2.

The crystalline size of F-N-TiO_2(1:6)-300 is larger than that of N-TiO_2 (4 h), indicating that NH_4F improves the growth of F-N-TiO_2(1:6)-300 grains. In order to confirm the result, we measured the BET specific surface area of F-N-TiO_2(a:b)-300 (Table 2). With increase of the ratio of a:b, the specific surface area decreases, which confirms further that NH_4F improves the growth of F-N-TiO_2(1:6)-300 grains.

Table 1
Crystalline size of various samples calculated by XRD data in Fig. 1.

Sample	Crystalline size (nm)
TiO_2	9.30
N-TiO_2	11.86
N-TiO_2 (4 h)	12.55
F-N-TiO_2(1:6)-300	12.91

Table 2
Specific surface area of various samples.

Sample	Specific surface area ($m^2\ g^{-1}$)
N-TiO_2	81.4
N-TiO_2 (4 h)	75.7
F-N-TiO_2(1:15)-300	70.3
F-N-TiO_2(1:6)-300	67.1
F-N-TiO_2(1:1)-300	51.6

3.1.2. Chemical states of doping nitrogen and fluorine

Fig. 3 shows FT-IR spectra of TiO_2, N-TiO_2 (4 h) and F-N-TiO_2(1:6)-300. For F-N-TiO_2(1:6)-300, no peak at 889.0 cm^{-1} is detected, which can be attributed to Ti–F vibration [23]. This suggests that fewer F^- ions could be doped into TiO_2 and the ions might be highly dispersive, in good agreement with the result from Fig. 2. Compared to TiO_2, the appearance of a new absorption peak at 1057 cm^{-1} for N-TiO_2 (4 h) and F-N-TiO_2(1:6)-300, which can be assigned to the N–Ti–O stretching vibration [24,25], indicates that some nitrogen atoms enter TiO_2 crystal lattice. Compared to TiO_2, two new absorption peaks appear at ca. 3132/3156 cm^{-1} and 1400 cm^{-1} respectively for N-TiO_2 (4 h) and F-N-TiO_2(1:6)-300. The two peaks correspond to the N–H stretching vibration and the N–H bending vibration of NH_4^+ respectively [26], indicating that there is a small amount of NH_4^+ on TiO_2. The absorption bands in the regions of 3434–3449 cm^{-1} and 1618–1632 cm^{-1} are assigned to the stretching vibration and bending vibration of the hydroxyl on the surface of TiO_2 catalyst respectively [27,28]. The larger vibration shift at 3434 and 1632 cm^{-1} for F-N-TiO_2(1:6)-300 could be due to the formation of stronger hydrogen bonds by the F^- ions compared to the corresponding peak positions of N-TiO_2 (4 h) and TiO_2.

Fig. 4 shows the high-resolution N1s spectra of F-N-TiO_2(1:6)-300 (a) and N-TiO_2 (b). Compared to the spectrum of N-TiO_2 (b), a small shoulder peak centered at 397.3 eV occurs for F-N-TiO_2(1:6)-300, which can be ascribed to formation of a Ti–N bond in TiO_2 [2]. This suggests that a small amount of nitrogen replaces the lattice oxygen of TiO_2 after the NH_4F treatment. Both F-N-TiO_2(1:6)-300 (a) and N-TiO_2 (b) show stronger peaks at ca. 400 eV. Romero-Gómez et al. [29] assigned the N1s peak at ca. 400 eV as the peak Ti–N–O local structure. Based on XPS and IR analyses, we conclude that both NH_4^+ species and Ti–N–O bonds exist on/in F-N-TiO_2(1:6)-300 and N-TiO_2.

The binding energy of N1s of NH_4^+ species is 401.7 ± 0.5 eV [30]. Although the intensity of F-N-TiO_2(1:6)-300 (a) at 399.9 eV is close to that of N-TiO_2 (b) at 400.2 eV, the peak position for F-N-TiO_2(1:6)-300 shifts to a lower value (from 400.2 eV to 399.9 eV) compared to that of N-TiO_2. This indicates that for F-N-TiO_2(1:6)-300 there are more Ti–N–O bonds in the lattice but fewer NH_4^+

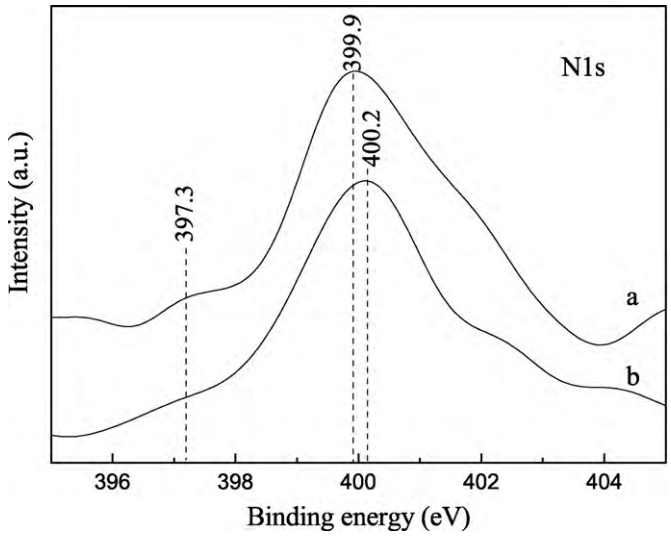

Fig. 4. N 1s XPS spectra of F-N-TiO_2(1:6)-300 (a) and N-TiO_2 (b).

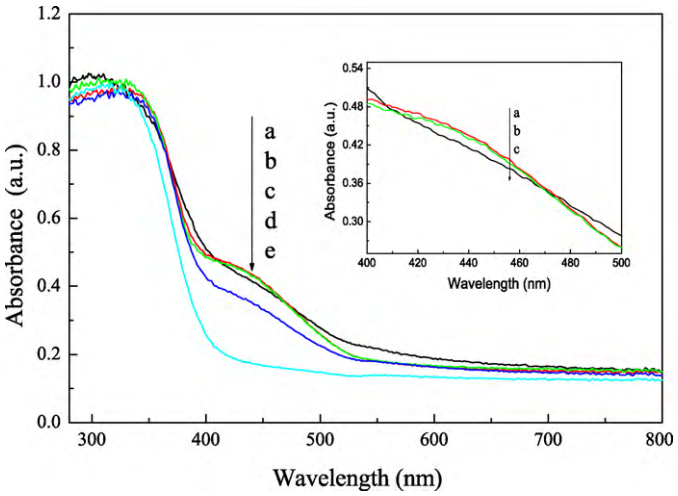

Fig. 6. UV–vis absorption spectra of F-N-TiO_2(*a*:*b*)-300 samples. (a) F-N-TiO_2(1:1), (b) F-N-TiO_2(1:6), (c) F-N-TiO_2(1:15), (d) N-TiO_2 and (e)TiO_2.

species on the surface, while for N-TiO_2 there are more NH_4^+ species on the surface but fewer Ti–N–O bonds in the lattice. This result shows that for F-N-TiO_2(1:6)-300, extra nitrogen is primarily doped in the form of Ti–N–O except for a small amount of nitrogen in the form of Ti–N bonds due to the NH_4F treatment.

Fig. 5 gives the high-resolution F1s XPS spectrum of F-N-TiO_2(1:6)-300. A stronger peak located at 684.4 eV corresponds to F^- ions physically adsorbed on TiO_2 [18]. A weaker peak located at 689.8 eV is assigned to F^- ions in Ti–F bonds [31], indicating that a small amount of F^- should be doped into the TiO_2 lattice or at the surface after the treatment of NH_4F.

3.1.3. Photoabsorption performance

Fig. 6 shows the UV–vis absorption spectra of F-N-TiO_2(*a*:*b*)-300 samples. The absorption of TiO_2 (sample e) is limited only to ultraviolet light region, while the absorption threshold values of N-TiO_2 (sample d) and F-N-TiO_2 (samples a–c) are extended up to ca. 535 nm. The absorption intensities of F-N-TiO_2(1:1) (sample a), F-N-TiO_2(1:6) (sample b) and F-N-TiO_2(1:15) (sample c) are almost identical between 400–500 nm (centered at ca. 450 nm) (inset of Fig. 6). However, compared to the absorption intensity of N-TiO_2 (sample d), those of the three F-N-TiO_2(*a*:*b*) samples increase. Compared to the baseline of TiO_2, that of N-TiO_2 elevates markedly. It is interesting that the baselines of samples a and b are close to that of N-TiO_2, while the baseline of sample c is much higher than that of N-TiO_2.

Lin et al. [32], combining theoretical calculations with the analysis of UV–vis spectra, concluded that the optical absorption of N-doped TiO_2 is located between 400 and 500 nm, while that of oxygen-deficient TiO_2 appears above 500 nm. In relation with our results, we can tentatively assume that elevation of baselines for sample N-TiO_2 and the three F-N-TiO_2(*a*:*b*) samples, depicting a broad absorption at $\lambda > 500$ nm, presents a considerable concentration of oxygen vacancies and other defects in the structure of TiO_2. Meanwhile, the absorption features at around 450 nm found in samples a, b, c and d are likely related with absorption centers associated to nitrogen incorporated within the structure of the titanium oxide.

The increase in the absorption of samples a, b and c between 400 and 535 nm can be ascribed to further nitrogen doping by NH_4F treatment. The different baseline levels of the samples a, b, c compared to N-TiO_2 suggest that the concentration of oxygen vacancies in sample c is higher than that in N-TiO_2, whereas the concentrations in samples a and b are close to that in N-TiO_2 due to doped fluorine reducing oxygen vacancies (see Section 4).

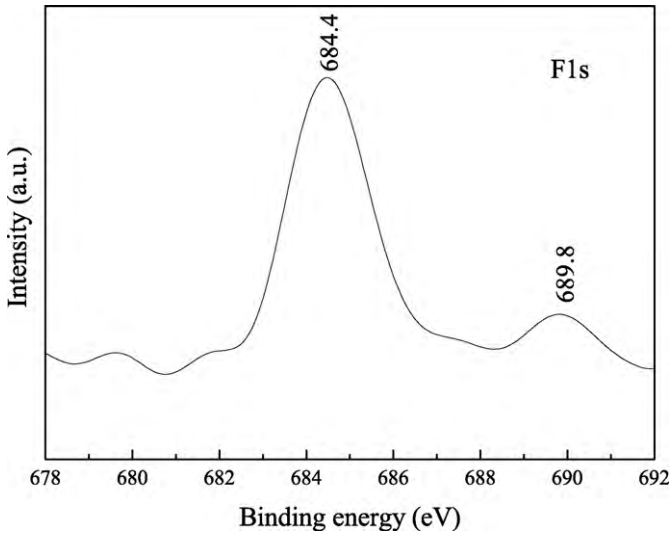

Fig. 5. F1s XPS spectrum of F-N-TiO_2(1:6)-300.

3.1.4. Photoactivity of F-N-TiO_2(*a*:*b*)-300

Fig. 7 displays time curves of photocatalytic degradation of formaldehyde over various samples calcined at 300 °C under blue LED irradiation. The blank experiment (curve b) shows that after formaldehyde was injected into the reactor for 0.5 h under no light irradiation, the formaldehyde concentration decreases by 15%. The decrease can be attributed to the sorption of formaldehyde molecules on the inner wall of the reactor and on the glass surface. Similarly, a decrease of the formaldehyde concentration (curve a) before irradiation is also attributable to the sorption of formaldehyde molecules on the inner wall of the reactor and on the TiO_2 photocatalyst film. After irradiation, no remarked decrease of the formaldehyde concentration occurs (curve a), which is ascribable to TiO_2 not being able to absorb blue light and thus photocatalytic degradation of formaldehyde cannot take place. N-TiO_2, F-N-TiO_2(1:15), F-N-TiO_2(1:1) and F-N-TiO_2(1:6) exhibit obvious visible-light activities for photocatalytic degradation of formaldehyde. All N-TiO_2 modified with NH_4F (F-N-TiO_2(1:15), F-N-TiO_2(1:1) and F-N-TiO_2(1:6)) have better activities than that

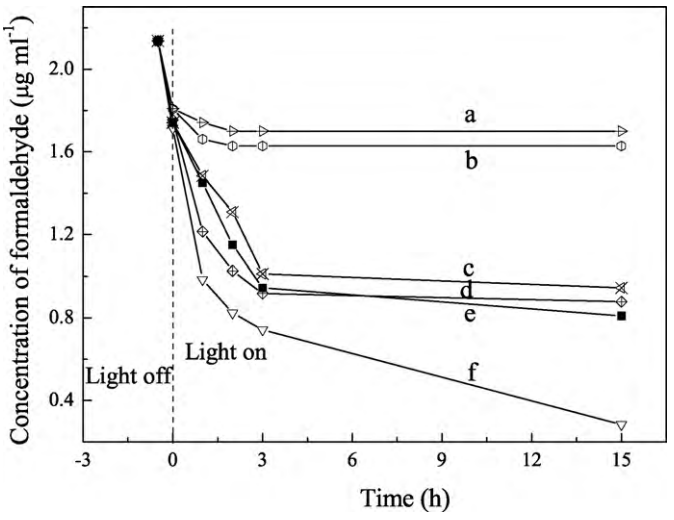

Fig. 7. Time curves of formaldehyde degradation over various photocatalyst samples calcined at 300 °C under blue LED irradiation. (a) TiO_2, (b) blank, (c) N-TiO_2, (d) F-N-TiO_2(1:15), (e) F-N-TiO_2(1:1) and (f) F-N-TiO_2(1:6).

of N-TiO_2, which can be attributed to higher visible absorption due to the further nitrogen doping (Fig. 6). Among the three F-N-TiO_2 samples, F-N-TiO_2(1:6) exhibits the highest activity for the degradation of formaldehyde (87% of degradation rate for 15 h irradiation), which is due to increased visible absorption by the further nitrogen doping, and to reduced oxygen vacancies by the fluorine doping. The activity of F-N-TiO_2(1:15) is much lower than that of F-N-TiO_2(1:6), because there are more oxygen vacancies in F-N-TiO_2(1:15) (Fig. 6). The activity of F-N-TiO_2(1:1) is much lower than that of F-N-TiO_2(1:6), due to the smaller specific surface area (Table 2).

3.2. Effect of temperature for NH_4F modification

Fig. 8 shows UV–vis absorption spectra of F-N-TiO_2(1:6) calcined at different temperatures and TiO_2 calcined at 300 °C. The calcination temperature has a great influence on the optical absorption. The absorption intensities of F-N-TiO_2(1:6) samples in the region of ca. 400–535 nm decrease in the order of 400 °C > 300 °C ≫ 550 °C. With temperature increasing, more nitrogen could be doped into N-TiO_2. Thus, the absorption intensity of F-N-TiO_2(1:6)-400 is larger

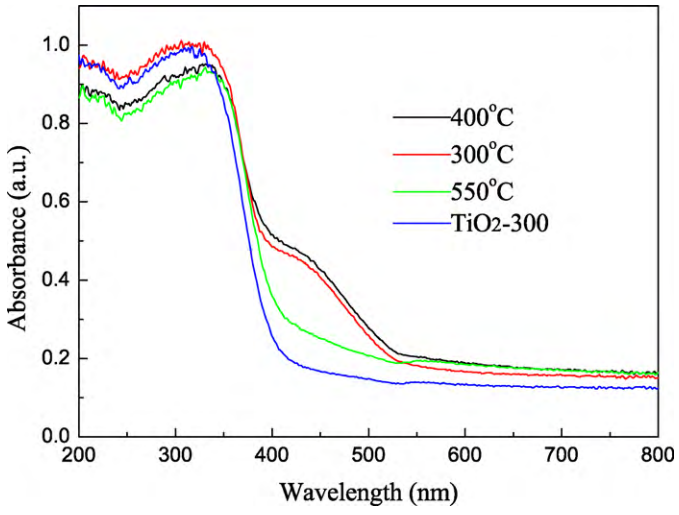

Fig. 8. UV–vis absorption spectra of F-N-TiO_2(1:6) calcined at different temperatures.

Table 3
Specific surface area of F-N-TiO_2(1:6) calcined at different temperatures.

Sample	Specific surface area ($m^2\ g^{-1}$)
F-N-TiO_2(1:6)-300	67.1
F-N-TiO_2(1:6)-400	39.7
F-N-TiO_2(1:6)-550	19.9

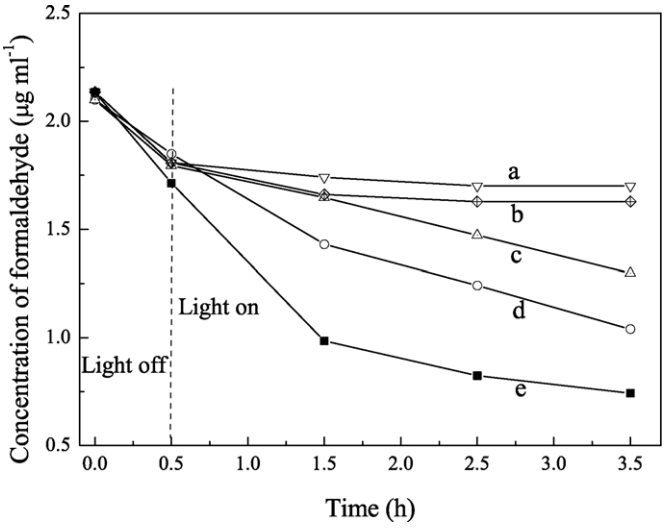

Fig. 9. Time curves of formaldehyde degradation over F-N-TiO_2(1:6) samples calcined at different temperatures under blue LED irradiation. (a) TiO_2-300, (b) blank, (c) F-N-TiO_2(1:6)-550, (d) F-N-TiO_2(1:6)-400 and (e) F-N-TiO_2(1:6)-300.

than that of F-N-TiO_2(1:6)-300. With further increase of temperature, release of the doped nitrogen would be accelerated by an oxidative reaction under air atmosphere [33]. Thus, the absorption intensity of F-N-TiO_2(1:6)-550 is the lowest.

Table 3 shows BET specific surface area of F-N-TiO_2(1:6) calcined at different temperatures. With increase of temperature, the specific surface area decreases markedly, which can be attributed to effect of temperature and stronger effect of NH_4F on the growth of F-N-TiO_2(1:6) grains at higher temperatures.

Fig. 9 displays time curves of photocatalytic degradation of formaldehyde over F-N-TiO_2(1:6) samples calcined at different temperatures under blue LED irradiation. With the temperature increasing, photocatalytic activities of F-N-TiO_2(1:6) samples decrease in the order of F-N-TiO_2(1:6)-300 > F-N-TiO_2(1:6)-400 > F-N-TiO_2(1:6)-550. F-N-TiO_2(1:6)-300 exhibits the highest activity due to higher visible absorption and the largest specific surface area, while F-N-TiO_2(1:6)-550 has the lowest activity due to the smallest visible absorption and specific surface area (Fig. 8 and Table 3). Although F-N-TiO_2(1:6)-400 has the largest visible absorption, its activity is much lower than that of F-N-TiO_2(1:6)-300, which can be attributed to the specific surface area of F-N-TiO_2(1:6)-400 being much smaller than that of F-N-TiO_2(1:6)-300.

4. Discussion

N doping into TiO_2 can produce oxygen vacancies [17], thus the baseline of sample d (N-TiO_2) elevates (Fig. 6). Due to the oxygen vacancies, nitrogen could be easily doped into samples a, b and c, which leads to an increase in their absorption between 400 and 535 nm. Because the absorption intensities of samples a, b and c are almost identical, nitrogen could easily be doped further to create a saturated nitrogen doping amount. Although nitrogen could be further doped into the samples with the treatment of NH_4F, the baselines of samples a and b are close to that of sample d, which

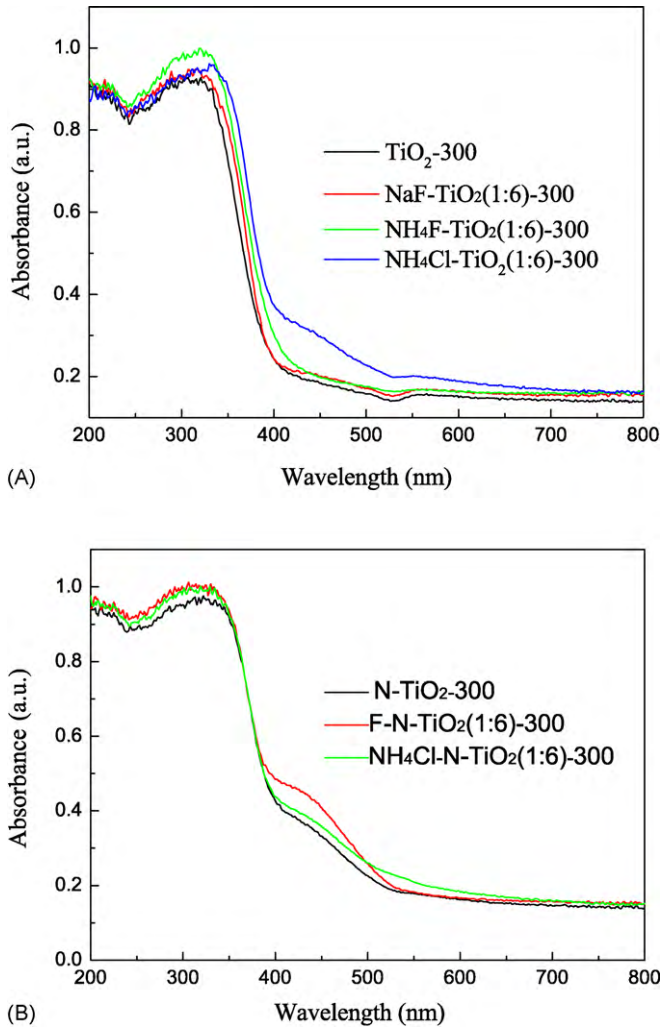

Fig. 10. UV–vis absorption spectra of various samples calcined at 300 °C.

could be attributed to that F^- co-doping into TiO_2 crystal lattice to remove oxygen vacancies by charge compensation. The reaction can be expressed as follows.

$$2O_O + NH_4^+(s) + F^-(s) = N_O' + F_O^\bullet + 2H_2O(g) \quad (3)$$

where O_O represents O^{2-} in a normal lattice site, N_O' represents N^{3-} in an O^{2-} lattice site, and $F_O^\bullet$ represents F^- in an O^{2-} lattice site. However, the baseline of sample c (F-N-TiO_2(1:15)) is higher than that of sample d (N-TiO_2) (Fig. 6). This could be ascribed to that fewer F^- ions entered the crystal lattice due to the smaller ratio of NH_4F to N-TiO_2, which could not effectively reduce the oxygen vacancies. Because of a large amount of hydroxyls on TiO_2 surface [34], NH_4^+ and F^- can be adsorbed on the surface by hydrogen bond. Hydrogen bond between F^- and the surface hydroxyl is much stronger than that between NH_4^+ and the hydroxyl. Thus, nitrogen can be doped easily, while fluorine doping is difficult. However, when NH_4F was excessive (the ratio of NH_4F to N-TiO_2 was larger), hydrogen bond does not markedly influence F^- doping anymore. Thus, F^- can be doped into samples a and b, while F^- cannot be effectively doped into sample c.

Fig. 10A shows the UV–vis absorption spectra of TiO_2 treated by NaF, NH_4F and NH_4Cl at 300 °C. The absorption spectrum of NaF-TiO_2(1:6)-300 is close to that of TiO_2-300, indicating that F-doping cannot produce remarked visible absorption, which is in good agreement with the reported result [35]. The absorption spectrum of NH_4F-TiO_2(1:6)-300 is also close to that of TiO_2-300 and there is no absorption peak between 400 and 535 nm for NH_4F-TiO_2(1:6)-300, indicating that nitrogen cannot be doped into TiO_2 by treatment of NH_4F. This result is very different from nitrogen doping into N-TiO_2 by treatment of NH_4F (Fig. 6). However, there is a stronger absorption peak between 400 and 535 nm for NH_4Cl-TiO_2(1:6)-300, indicating that nitrogen can be doped into TiO_2 by treatment of NH_4Cl.

The radius of F^- ion (136 pm) is close to that of O^{2-} ion (140 pm), while radius of Cl^- ion (181 pm) is much larger than that of O^{2-} ion. Thus, F^- ions can be doped into TiO_2 lattice, while Cl^- ions cannot. When TiO_2 was treated with NH_4Cl, nitrogen can be doped into TiO_2 lattice to form a large amount of oxygen vacancies which could improve further nitrogen doping. This can be confirmed by the elevated baseline. Thus, for NH_4Cl-TiO_2(1:6)-300, a stronger absorption peak between 400 and 535 nm occurs. However, when TiO_2 was treated with NH_4F, nitrogen doping and fluorine doping could take place at the same time as shown in reaction (3), and oxygen vacancies cannot be formed. Thus, further nitrogen doping was inhibited for NH_4F-TiO_2(1:6)-300. Because there are many oxygen vacancies for N-TiO_2, when it was modified with NH_4F, nitrogen can be doped further and the absorption intensity between 400 and 535 nm increases.

Fig. 10B shows the UV–vis absorption spectra of N-TiO_2 treated by NH_4F and NH_4Cl at 300 °C. The absorption intensities of F-N-TiO_2(1:6)-300 and NH_4Cl-N-TiO_2(1:6)-300 between 400 and 535 nm increase compared to that of N-TiO_2. However, the baseline level of NH_4Cl-N-TiO_2(1:6)-300 is higher than that of N-TiO_2, while the baseline level of F-N-TiO_2(1:6)-300 is close to that of N-TiO_2. This result confirms further that F-doping decreases the oxygen vacancies produced by nitrogen doping. The absorption intensity of NH_4Cl-N-TiO_2(1:6)-300 is much lower than that of F-N-TiO_2(1:6)-300, which can be attributed to the assumption that the excessive oxygen vacancies in NH_4Cl-N-TiO_2(1:6)-300 would inhibit further nitrogen doping. This implies that suitable fluorine doping would also improve further nitrogen doping.

Based on above results, we can conclude that oxygen vacancies produced by previous nitrogen doping for N-TiO_2, can improve further nitrogen doping when N-TiO_2 is modified by NH_4F; while fluorine doping by the modification of NH_4F can remove the oxygen vacancies derived from the further nitrogen doping.

F-doping into TiO_2 can create surface oxygen vacancies [35]. With increase of the calcination temperature, F^- ions could be doped into TiO_2 more easily. Thus, excessive F^- ions could be doped into TiO_2 lattice at higher temperature, which led to an increase of oxygen vacancy concentration instead of reducing the concentration. Compared to the absorption intensity of F-N-TiO_2(1:6)-300 above ca. 535 nm, the absorption intensities of F-N-TiO_2(1:6)-400 and F-N-TiO_2(1:6)-550 increase (Fig. 8), confirming the above assumption. Thus, excessive oxygen vacancies for F-N-TiO_2(1:6)-400 and F-N-TiO_2(1:6)-550 would decrease their photocatalytic activity, which could be another reason that they have lower activity.

5. Conclusions

N-TiO_2 was treated with NH_4F by an impregnation-calcination method and the NH_4F treatment enhances markedly photocatalytic activity of N-TiO_2. The treatment increases the visible absorption of N-TiO_2, decreases its specific surface area and influences the concentration of oxygen vacancies in N-TiO_2. The increase of the absorption can be attributed to further nitrogen doping due to oxygen vacancies derived from previous nitrogen doping; whereas fluorine doping can decrease the defects. Photocatalytic activity of F-N-TiO_2 depends on the visible absorption, the specific surface area, and the concentration of oxygen vacancies. The preparation

conditions, such as the calcination temperature and the initial molar ratio of NH_4F to N-TiO_2, have a significant influence on the photocatalytic activity. The optimum preparation condition for the high-activity photocatalyst is that the initial molar ratio of NH_4F to N-TiO_2 and the calcination temperature are 1:6 and 300 °C, respectively.

Acknowledgements

The financial supports of Program for Changjiang Scholars and Innovative Research Team in University (IRT0730), National Basic Research Program of China (2009CB220003), the National Nature Science Foundation of China (No.20763006), and Research Fund of Education Ministry of Jiangxi, China (GJJ09041) are gratefully acknowledged.

References

[1] A. Fujishima, T.N. Rao, D.A. Tryk, Titanium dioxide photocatalysis, J. Photochem. Photobiol. C 1 (2000) 1–21.
[2] R. Asahi, T. Morikawa, T. Ohwaki, K. Aoki, Y. Taga, Visible-light photocatalysis in nitrogen-doped titanium oxides, Science 293 (2001) 269–271.
[3] M.H. Zhou, J.G. Yu, Preparation and enhanced daylight-induced photocatalytic activity of C, N, S-tridoped titanium dioxide powders, J. Hazard. Mater. 152 (2008) 1229–1236.
[4] T. Ihara, M. Miyoshi, Y. Iriyama, O. Matsumoto, S. Sugihara, Visible-light-active titanium oxide photocatalyst realized by an oxygen-deficient structure and by nitrogen doping, Appl. Catal. B 42 (2003) 403–409.
[5] Y.X. Li, G.F. Ma, S.Q. Peng, G.X. Lu, S.B. Li, Photocatalytic H_2 evolution over basic zincoxysulfide ($ZnS_{1-x-0.5y}O_x(OH)_y$) under visible light irradiation, Appl. Catal. A 363 (2009) 180–187.
[6] Y.X. Li, G.F. Ma, S.Q. Peng, G.X. Lu, S.B. Li, Boron and nitrogen co-doped titania with enhanced visible-light photocatalytic activity for hydrogen evolution, Appl. Surf. Sci. 254 (2008) 6831–6836.
[7] K.L. Lv, H.S. Zuo, J. Sun, K.J. Deng, S.C. Liu, X.F. Li, D.Y. Wang, (Bi, C and N) codoped TiO_2 nanoparticles, J. Hazard. Mater. 161 (2009) 396–401.
[8] S.W. Liu, J.G. Yu, S. Mann, Synergetic codoping in fluorinated $Ti_{1-x}Zr_xO_2$ hollow microspheres, J. Phys. Chem. C 113 (2009) 10712–10717.
[9] T. Ohno, M. Akiyoshi, T. Umebayashi, K. Asai, T. Mitsui, M. Matsumura, Preparation of S-doped TiO_2 photocatalysts and their photocatalytic activities under visible light, Appl. Catal. A 265 (2004) 115–121.
[10] K. Kobayakawa, Y. Murakami, Y. Sato, Visible-light active N-doped TiO_2 prepared by heating of titanium hydroxide and urea, J. Photochem. Photobiol. A: Chem. 170 (2005) 177–179.
[11] C. Burda, Y.B. Lou, X.B. Chen, A.C.S. Samia, J. Stout, J.L. Gole, Enhanced nitrogen doping in TiO_2 nanoparticles, Nano. Lett. 3 (2003) 1049–1051.
[12] S. Yin, K. Ihara, M. Komatsu, Q.W. Zhang, F. Saito, T. Kyotani, T. Sato, Low temperature synthesis of $TiO_{2-x}N_y$ powders and films with visible light responsive photocatalytic activity, Solid State Commun. 137 (2006) 132–137.
[13] D. Li, H. Haneda, S. Hishita, N. Ohashi, Visible-light-driven nitrogen-doped TiO_2 photocatalysts: effect of nitrogen precursors on their photocatalysis for decomposition of gas-phase organic pollutants, Mater. Sci. Eng. B 117 (2005) 67–75.
[14] H. Irie, Y. Watanabe, K. Hashimoto, Nitrogen-concentration dependence on photocatalytic activity of $TiO_{2-x}N_x$ powders, J. Phys. Chem. B 107 (2003) 5483–5486.
[15] X.M. Fang, Z.G. Zhang, Q.L. Chen, H.B. Ji, X.N. Gao, Dependence of nitrogen doping on TiO_2 precursor annealed under NH_3 flow, J. Solid State Chem. 180 (2007) 1325–1332.
[16] Z.B. Wu, F. Dong, W.R. Zhao, S. Guo, Visible light induced electron transfer process over nitrogen doped TiO_2 nanocrystals prepared by oxidation of titanium nitride, J. Hazard. Mater. 157 (2008) 57–63.
[17] C.D. Valentin, E. Finazzi, G. Pacchioni, A. Selloni, S. Livraghi, M.C. Paganini, E. Giamello, N-doped TiO_2: theory and experiment, Chem. Phys. 339 (2007) 44–56.
[18] J.C. Yu, J.G. Yu, W. Ho, Z. Jiang, L. Zhang, Effects of F^- doping on the photocatalytic activity and powders microstructures of nanocrystalline TiO_2, Chem. Mater. 14 (2002) 3808–3816.
[19] A. Hattori, K. Shimota, H. Tada, S. Ito, Photoreactivity of sol-gel TiO_2 films formed on soda-lime glass substrates: effect of SiO_2 underlayer containing fluorine, Langmuir 15 (1999) 5422–5425.
[20] J.G. Yu, X.J. Zhao, J.C. Du, W.M. Chen, Preparation, microstructure and photocatalytic activity of the porous TiO_2 anatase coating by sol-gel processing, J. Sol–Gel Sci. Technol. 17 (2000) 163–171.
[21] Y.X. Li, J. Du, S.Q. Peng, G.X. Lu, S.B. Li, Enhancement of photocatalytic activity of cadmium sulfide for hydrogen evolution by photoetching, Int. J. Hydrogen Energy 33 (2008) 2007–2013.
[22] "Air quality-determination of formaldehyde-acetylacetone spectrophotometric method" Chinese national standard GB/T 15516-1995.
[23] D.G. Huang, S.J. Liao, D. Zhi, Preparation, characterization and photocatalytic performance of anatase F doped TiO_2 sol, Acta Chim. Sin. 64 (2006) 1805–1811.
[24] S. Liu, X. Chen, X. Chen, N-doped visible light response nanosize TiO_2 photocatalyst prepared by acid catalyzed hydrolysis method, Chin. J. Catal. 27 (2006) 697–702.
[25] Y.X. Li, C.F. Xie, S.Q. Peng, G.X. Lu, S.B. Li, Eosin Y-sensitized nitrogen-doped TiO_2 for efficient visible light photocatalytic hydrogen evolution, J. Mol. Catal. A: Chem. 282 (2008) 117–123.
[26] T. Matsumoto, N. Iyi, Y. Kaneko, K. Kitamura, S. Ishihara, Y. Takasu, Y. Murakami, High visible-light photocatalytic activity of nitrogen-doped titania prepared from layered titania/isostearate nanocomposite, Catal. Today 120 (2007) 226–232.
[27] J.G. Yu, X.J. Zhao, Q. Zhao, Effects of surface morphology of photocatalytic porous TiO_2 thin films on hydrophilicity, J. Chin. Ceram. Soc. 28 (2000) 245–250.
[28] D. Zhang, X. Hu, T. Li, Y. Huang, Y. Ma, L. Li, Study on the microstructure and the optical capability of the nano-TiO_2 film, Acta Photonica Sinica 33 (2004) 982–985.
[29] P. Romero-Gómez, V. Rico, A. Borrás, A. Barranco, J.P. Espinós, J. Cotrino, A.R. González-Elipe, Chemical state of nitrogen and visible surface and schottky barrier driven photoactivities of N-doped TiO_2 thin films, J. Phys. Chem. C 113 (2009) 13341–13351.
[30] B. Gong, P.J. Pigram, R.N. Lamb, Identification of inorganic nitrogen in an Australian bituminous coal using x-ray photoelectron spectroscopy (XPS) and time-of-flight secondary ion mass spectrometry (TOFSIMS), Int. J. Coal Geol. 34 (1997) 53–68.
[31] X.Q. Chen, Y.L. Su, X.W. Zhang, L.C. Lei, Fabrication of visible-light responsive S-F-codoped TiO_2 nanotubes, Chin. Sci. Bull. 53 (2008) 1983–1987.
[32] Z. Lin, A. Orlov, R.M. Lambert, M.C. Payne, New insights into the origin of visible light photocatalytic activity of nitrogen-doped and oxygen-deficient anatase TiO_2, J. Phys. Chem. B 109 (2005) 20948–20952.
[33] M. Sathish, B. Viswanathan, R.P. Viswanath, C.S. Gopinath, Synthesis, characterization and photocatalytic activity of nitrogen doped TiO_2 nanocatalyst, Chem. Mater. 17 (2005) 6349–6353.
[34] Y.X. Li, G.X. Lu, S.B. Li, Photocatalytic hydrogen generation and decomposition of oxalic acid over platinized TiO_2, Appl. Catal. A 214 (2001) 179–185.
[35] D. Li, N. Ohashi, S. Hishita, T. Kolodiazhnyi, H. Haneda, Origin of visible-light-driven photocatalysis: A comparative study on N/F-doped and F-N-codoped TiO_2 powders by means of experimental characterizations and theoretical calculations, J. Solid State Chem. 178 (2005) 3293–3302.